1963ApJ...137.1057S

A FOUR-COLOR PHOTOMETRIC SYSTEM APPLIED TO LINE BLANKETING OF SUBDWARFS

ALLAN SANDAGE AND LEWIS L. SMITH
Mount Wilson and Palomar Observatories
Carnegie Institution of Washington, California Institute of Technology
Received December 24, 1962

ABSTRACT

Photoelectric observations made with a multialkali RCA C7237 photomultiplier (S20 surface) are reported for 96 stars. The usual U, B, V band passes were measured, plus an r point at $\bar{\lambda} = 6700$ A. Conventional U, B, V values were available for nearly all 96 stars, and comparison with our S20 system reduced by linear transformation to $U - B$, $B - V$ colors, shows that multialkali cathodes can reproduce $B - V$ colors with good accuracy and $U - B$ colors with moderate accuracy.

The subdwarfs observed on the program are shown to be separated from strong-lined, Hyades-like stars in both the $U - B$, $v - r$ and the $B - V$, $v - r$ two-color diagrams The blanketing theory, extended to the $v - r$ color, shows that the color changes $\Delta(U - B)$, $\Delta(B - V)$, and $\Delta(v - r)$ predicted for each program star completely eliminates the separation of the subdwarfs from the Hyades-like stars in the two-color diagrams.

Previous results, together with the present study, show that the observed colors of a typical globular cluster subdwarf at the main-sequence termination point must be made redder by $\Delta(U - B) = 0\overset{m}{.}40$. $\Delta(B - V) = 0\overset{m}{.}18$, $\Delta(v - r) = 0\overset{m}{.}04$, and $\Delta(G - I)$ of the Stebbins-Whitford six-color system $= 0\overset{m}{.}00$, before comparison with Hyades-like stars can be made, which emphasizes the well-known result that broad-band photometry should be done in the red to minimize the effects of Fraunhofer-line blanketing.

I. INTRODUCTION

The recent availability of photomultipliers with type S20 cathodes which are sensitive from λ 3000 A to λ 8000 A suggests that present routine three-color photometry might conveniently be extended to include a red point near λ 6700 A. This paper reports observations made in the summer of 1960 with the Palomar 20-inch reflector using an experimental RCA C7237 multiplier refrigerated with dry ice and operated at 1300 volts accelerating potential. This tube has since gone into commercial production as RCA type 7265. It is a fourteen-stage, end-on photomultiplier with a multialkali cathode.

Two experimental programs were undertaken with the multiplier. (1) Many standard stars of the U, B, V photometric system (Johnson and Morgan 1953; Johnson and Harris 1954) were observed to see how well the S20 surface can reproduce $U - B$ and $B - V$ colors. At the same time, a fourth color at $\bar{\lambda} \simeq 6700$ A was added. (2) The four-color system was used to observe a number of stars which have extremely weak Fraunhofer lines, so as to check and to extend the methods recently developed to correct U, B, V data for differential line blanketing (Code 1959; Sandage and Eggen 1959; Melbourne 1960; Smak 1960; Wildey, Burbidge, Sandage, and Burbidge 1962).

II. FOUR-COLOR OBSERVATIONS OF STARS WHICH DEFINE THE U, B, V SYSTEM

a) *The Photometric System*

The spectral response of the multialkali photometer is shown in Figure 1. The choice of filters presented some difficulties because of the red leak of the usual ultraviolet and blue glass. After considerable experimentation, we adopted 2.8 mm of Corning 9863 for the ultraviolet filter, but with the addition of a 2.5-mm-thick liquid chamber, which, following Gehrels and Teska (1960), was filled with an 80 per cent saturated solution of $CuSO_4 \cdot 5H_2O$. This arrangement completely suppressed the red leak of the 9863 glass alone (see Kasha 1948 for the transmission function of $CuSO_4$). The blue filter was a sandwich of 0.7 mm of Schott BG12 plus 2 mm of GG13, a combination which also has a slight red leak that was again suppressed by a 2.5-mm liquid chamber filled with $CuSO_4$. The visual filter was a sandwich of 2.2 mm of Schott GG11 with 1.6 mm of Schott BG18, a combination which closely matches the usual Corning 3384 or Schott GG11 used with a normal 1P21 multiplier. The red filter for the *r* point was 2 mm of Schott RG1. The cutoff on the red side of the band pass is provided by the S20 response of the cell.

Figure 1 was constructed from the manufacturer's quoted response of the RCA 7237 multiplier folded into the actual transmissions of the filter combinations as measured in

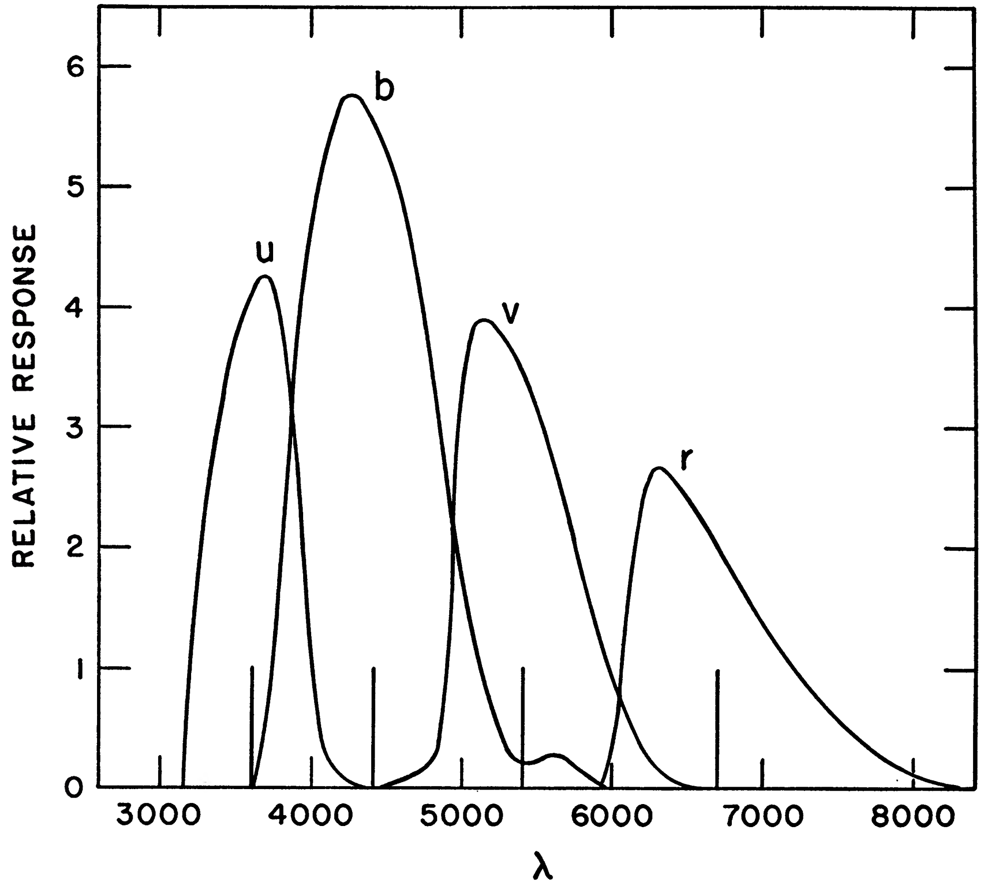

FIG. 1.—The transmission function $S(\lambda)$ for the filters, S20 photocathode, and two reflections from Al. The filters are 2.8 mm of Corning 9863 plus 2 5 mm of 80 per cent saturated $CuSO_4 \cdot 5\ H_2O$ solution for *u;* 0.7 mm of Schott BG12 plus 2 mm of Schott GG13 plus 2.5 mm of 80 per cent saturated $CuSO_4 \cdot 5\ H_2O$ solution for *b;* 1.6 mm of Schott BG18 plus 2.2 mm of Schott GG11 for *v;* and 2 mm of Schott RG1 for *r*.

the Mount Wilson laboratory. No attempt has been made to check the complete response-curves in the laboratory because measurements of real stars with the equipment are more germane to our present problem than knowledge of the precise $S(\lambda)$ of the theoretical system. Our later use of the theoretical $S(\lambda)$ functions does not require that they be known precisely.

b) Observations of Standard Stars

Sixty-four stars which are listed in the Johnson and Morgan (1953) and the Johnson and Harris (1954) catalogues were observed with the new equipment in July and September, 1960. Comparison of the colors obtained on the natural photometric system (reduced to outside the atmosphere) with the Johnson, Morgan, and Harris $U - B$, $B - V$ values gives

$$B - V = 1.100\,(b - v)_{20} + 1.023 \qquad (1)$$
$$\pm 0.004 \qquad\qquad \pm 0.003\,,$$

$$U - B = 1.015\,(u - b)_{20} - 1.575 \qquad (2)$$
$$\pm 0.003 \qquad\qquad \pm 0.006\,,$$

where $(b - v)_{20}$ and $(u - b)_{20}$ refer to natural colors obtained with the S20 cathode. The slope coefficients of equations (1) and (2) show that our filter system is close to, but not identical with, the U, B, V system. This can also be shown theoretically by comparison of effective wavelengths. Matthews and Sandage (1963, Appendix A) have computed that $\bar{\lambda}_U = 3610$ A, $\bar{\lambda}_B = 4440$ A, and $\bar{\lambda}_V = 5545$ A for the U, B, V system with a source of equal energy at all λ (per unit wavelength interval). The data from which Figure 1 was constructed give $\bar{\lambda}_u = 3620$ A, $\bar{\lambda}_b = 4420$ A, and $\bar{\lambda}_v = 5400$ A for the multialkali photometer. These values require that $B - V = 1.094\,(b - v)_{20} +$ const. and $U - B = 1.037\,(u - b)_{20} +$ const. for the theoretical systems, which are in good agreement with equations (1) and (2).

The observational data, transformed by equations (1) and (2), are given in Table 1, where the notation $(B - V)_{20}$ and $(U - B)_{20}$ is used to distinguish between conventional 1P21 photometers and our S20 system. The suitability of the S20 surface for observing on the U, B, V system can now be tested by comparing Table 1 with the U, B, V defining values of Johnson, Morgan, and Harris. The results are shown in Figure 2, where the residuals are taken as $(B - V)_{\rm JM} - (B - V)_{20}$ and $(U - B)_{\rm JM} - (U - B)_{20}$. Closed circles are luminosity IV and V stars, open circles are class III stars, and triangles are class I stars. The $B - V$ residuals are small and are not correlated with color, which shows that multialkali surfaces can be used to produce $B - V$ colors with high accuracy. The $U - B$ residuals show a slight systematic variation with color, whose semiamplitude reaches $\pm 0^{\rm m}.02$, but we do not consider this to be established because when the additional data for the subdwarfs of Table 2, discussed in the next section, are compared with the conventional 1P21 photometric data for the same stars, the $U - B$ residuals are smaller than in Figure 2, and the systematic effect nearly disappears. Our complete data taken together suggest that $(U - B)_{20}$ colors for stars whose $B - V$ colors are redder than 0.50 do not systematically deviate by more than $0^{\rm m}.02$ from $(U - B)_{\rm JM}$ and that the deviations may even be smaller. In any case, the $(B - V)_{20}$ and $(U - B)_{20}$ colors are sufficiently close to $B - V$ and $U - B$ that they are used without further distinction in the remainder of the text and diagrams.

c) The v—r Colors

Table 1 gives our observed $(v - r)_{20}$ colors for the standard stars. We have adopted the conventional zero point such that $v - r = 0$ for stars with $U - B = B - V = 0.00$.[1] Figure 3 shows the correlation of $B - V$ with $v - r$ for stars of Table 1. Closed circles are stars of luminosity class IV or V, crosses are class III, and triangles are class I. A separation of giants and dwarfs probably occurs beginning at $B - V = 0.8$, but there are insufficient data to be certain. (The deviation of the luminosity class I stars from the other points is probably a result of interstellar reddening.)

[1] We have chosen to designate this color index by small letters so as to indicate that it is a natural system. At the present time we do not wish to suggest that $v - r$ has status as a standard system in future work because multialkali cells are not now in general use and it may indeed turn out that a wider base-line photomultiplier, such as the RCA 7102, will be more useful for the majority of problems. In this case, a different $v - r$ will prevail.

1963ApJ...137.1057S

TABLE 1

FOUR-COLOR DATA FOR STARS WHICH DEFINE THE U, B, V SYSTEM

JM No. (1)	HD (2)	Star Name (3)	Sp Type (4)	$(U-B)_{20}$ (5)	$(B-V)_{20}$ (6)	$(v-r)_{20}$ (7)	$\delta(U-B)$ (8)	n (9)
			PRIMARY STANDARDS					
145	135742	β Lib	B8 V	−0.37	−0.12	−0.10	.....	5
152	140573	α Ser	K2 III	+1.25	+1.16	+0.80	.....	5
158	143107	ϵ CrB	K3 III	+1.26	+1.22	+0.85	.....	9
165	147394	τ Her	B5 IV	−0.56	−0.15	−0.12	.....	7
270	214680	10 Lac	O9 V	−1.04	−0.20	−0.11	.....	29
279	219134	HR 8832	K3 V	+0.89	+1.01	+0.84	−0.03	25
			SECONDARY STANDARDS					
1	432	β Cas	F2 IV	+0.10	+0.36	+0.30	−0.07	3
13	6582	μ Cas	G5 Vp	+0.11	+0.70	+0.59	+0.15	5
17	9270	η Psc	G8 III	+0.73	+0.97	+0.69	.....	4
20	10307	HR 483	G2 V	+0.15	+0.65	+0.52	+0.04	2
22	10700	τ Cet	G8 Vp	+0.22	+0.73	+0.58	+0.08	3
28	13974	δ Tri	G0 V	+0.03	+0.61	+0.53	+0.12	2
38	19373	ι Per	G0 V	+0.12	+0.60	+0.49	+0.01	2
134	123299	α Dra	A0 III	−0.12	−0.07	−0.05	.....	1
138	126660	θ Boo	F7 V	+0.01	+0.48	+0.39	+0.01	1
139	127665	ρ Boo	K3 III	+1.42	+1.27	+0.92	.....	1
140	127762	γ Boo	A7 III	+0.10	+0.18	+0.13	.....	1
141	130109	109 Vir	A0 V	−0.05	−0.02	−0.02	.....	2
143	135722	δ Boo A	G8 III	+0.66	+0.95	+0.69	.....	1
144	......	δ Boo B	G0 V	0.00	+0.59	+0.46	+0.12	1
148	137391	μ Boo	F0 V	+0.04	+0.34	+0.25	0.00	1
149	137759	ι Dra	K2 III	+1.22	+1.18	+0.85	.....	2
150	139006	α CrB	A0 V	−0.04	0.00	−0.03	.....	1
151	140159	ι Ser	A1 V	+0.03	+0.06	+0.02	.....	1
155	141004	λ Ser	G0 V	+0.12	+0.60	+0.49	+0.01	2
156	142373	χ Her	F9 V	0.00	+0.55	+0.47	+0.08	1
157	142860	γ Ser	F6 V	−0.02	+0.47	+0.40	+0.03	1
162	144284	θ Dra	F8 IV-V	+0.11	+0.57	+0.43	0.00	1
166	147547	γ Her	A9 III	+0.16	+0.26	+0.20	.....	1
168	150680	ζ Her	G0 IV	+0.22	+0.65	+0.48	−0.03	1
175	157214	72 Her	G0 V	+0.09	+0.63	+0.49	+0.08	2
176	157881	Cin 2322	K7 V	+1.18	+1.34	+1.16	.....	1
183	161096	β Oph	K2 III	+1.22	+1.18	+0.82	.....	1
184	161797	μ Her A	G5 IV	+0.41	+0.77	+0.57	−0.03	1
186	161868	γ Oph	A0 V	+0.01	+0.04	0.00	.....	1
191	165908	99 Her	F7 V	−0.04	+0.54	+0.47	+0.11	2
197	170153	χ Dra	F7 V	−0.01	+0.51	+0.48	+0.05	1
201	173667	110 Her	F6 V	+0.04	+0.48	+0.40	−0.02	1
206	176437	γ Lyr	B9 III	−0.08	−0.04	+0.01	.....	1
215	185144	σ Dra	K0 V	+0.41	+0.82	+0.66	+0.07	1
216	186408	16 Cyg A	G2 V	+0.17	+0.64	+0.50	+0.01	2
217	186427	16 Cyg B	G5 V	+0.18	+0.65	+0.51	+0.01	2
224	188512	β Aql	G8 IV	+0.49	+0.85	+0.65	+0.05	2
230	195593	44 Cyg	F5 Iab	+0.69	+0.99	+0.83	.....	2
232	196867	α Del	B9 V	−0.20	−0.07	−0.02	.....	2
236	197989	ϵ Cyg	K0 III	+0.88	+1.06	+0.77	.....	1
237	198001	ϵ Aqr	A1 V	+0.02	+0.01	+0.02	.....	1
238	198149	η Cep	K0 IV	+0.64	+0.94	+0.71	.....	1
239	198478	55 Cyg	B3 Ia	−0.47	+0.40	+0.41	.....	2
244	203280	α Cep	A7 IV-V	+0.10	+0.23	+0.20	.....	3
249	206165	9 Cep	B2 Ib	−0.55	+0.28	+0.28	.....	2
260	210027	ι Peg	F5 V	−0.02	+0.44	+0.38	+0.02	2
261	210839	λ Cep	O6 f	−0.73	+0.26	+0.28	.....	1
264	211336	ϵ Cep	F0 IV	+0.07	+0.30	+0.26	0.00	1
271	215182	η Peg	G2 II-III	+0.57	+0.87	+0.65	.....	2
272	215648	ξ Peg	F7 V	−0.01	+0.51	+0.43	+0.05	2
274	216735	ρ Peg	A1 V	−0.04	−0.01	−0.02	.....	2
277	217476	HR 8752	G0 Ia	+1.06	+1.38	+1.05	.....	1
278	218329	55 Peg	M2 III	+1.87	+1.56	+1.27	.....	1
282	220657	υ Peg	F8 IV	+0.17	+0.60	+0.49	−0.04	2
283	222107	λ And	G8 III-IV	+0.71	+1.02	+0.82	.....	2
284	222368	ι Psc	F7 V	+0.01	+0.52	+0.43	+0.04	4
286	222439	$\varkappa$ And	B8 V	−0.24	−0.08	−0.08	.....	3
288	224930	85 Peg	G2 V	+0.07	+0.67	+0.58	+0.14	3

Note that the relation in Figure 3 is slightly non-linear in the same sense as in the conventional $U - B$, $B - V$ diagram. This is very likely the effect of the strong hydrogen lines in the b filter band near the Balmer limit, which depress the continuum in A and early F stars ($B - V \simeq 0.0$ to $B - V \simeq 0.50$).

III. THE OBSERVED TWO-COLOR DIAGRAMS AND THE BLANKETING EFFECT

One major reason for adding a red photometric point in routine stellar photometry is to minimize the effect of Fraunhofer line blanketing on broad-band colors. Only small blanketing corrections are expected in the red because of the relative paucity of lines beyond $\lambda \simeq 5500$ A. This expectation has been tested by observing selected subdwarfs in the general field which were known to have weak lines from previous work of Roman (1955) and Sandage (1963). The four-color data for these stars are given in Table 2. All

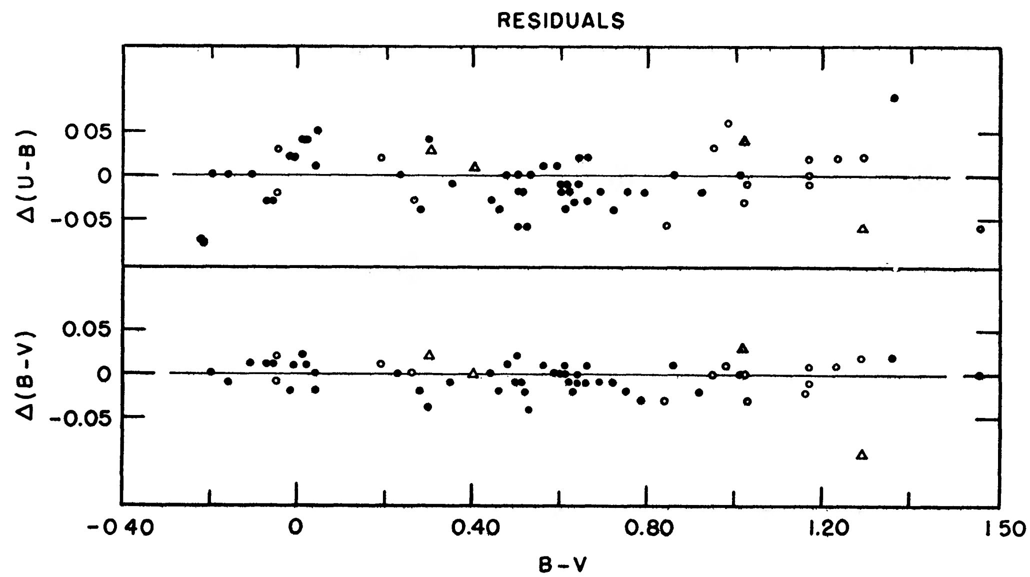

FIG 2—Comparison of our $(U - B)_{20}$, $(B - V)_{20}$ values with $U - B$, $B - V$ colors on the Johnson-Morgan U, B, V system The differences are in the sense Johnson-Morgan *minus* S20.

stars in Tables 1 and 2 of luminosity classes IV, V, and the subdwarfs are plotted in Figure 4, *a*, which gives the two-color diagram in the $U - B$, $v - r$ plane. The closed circles represent stars whose ultraviolet excesses are less than $0^{m}.05$, while the open circles are for stars with $\delta(U - B) \geq 0^{m}.05$. The separation of subdwarfs and normal stars is clearly present and is caused by the sum of the two blanketing vectors $\Delta(U - B)$ and $\Delta(v - r)$. The value of $\Delta(U - B)$ can be found from Table 4 of Wildey, Burbidge, Sandage, and Burbidge (1962, hereafter called "WBSB"), once $\delta(U - B)$ is known. The theory of $\Delta(v - r)$ is given in the next section, where it is shown that $\Delta(v - r)$ is not zero and, therefore, that the addition of only an r point to U, B, and V does not completely eliminate differential line blanketing, although $\Delta(v - r)$ is much smaller than either $\Delta(U - B)$ or $\Delta(B - V)$.

IV. THEORY OF THE $\Delta(v - r)$ BLANKETING

The corrections to U, B, V, and r caused by progressive weakening of the Fraunhofer lines are the sum of two terms, one due to blocking of the continuum by the absorption lines and the other due to the change in the continuum level due to radiation scattered back into the photosphere by the lines. As the lines are weakened in any given star, the radiation blocked by the lines becomes less, which allows more of the continuum radiation to emerge. However, less radiation is back-scattered, and the level of the continuum decreases, which tends to compensate for the blocking effect. The computation of ΔU, ΔB, and ΔV is discussed in detail by WBSB and will not be reproduced here.

We have obtained Δr for the same eight stars used by WBSB by assuming that the blocking term in Δr is zero, since there are few Fraunhofer lines in the r spectral region. Therefore, the back-warming term is the only contributor to Δr, and it is found by considering the two temperatures T_1 and T_2 which characterize the continuum level of a star with and without its normal Fraunhofer lines; T_1 is the effective temperature with which tables of model atmospheres must be entered to predict the level of the continuum of the star which has its given line strengths; T_2 is that temperature which will give the model-atmosphere continuum for the same star, once all the Fraunhofer lines are removed. Obviously, $T_1 > T_2$, and they are related by

$$T_2^4 = (1 - \eta) T_1^4 , \tag{3}$$

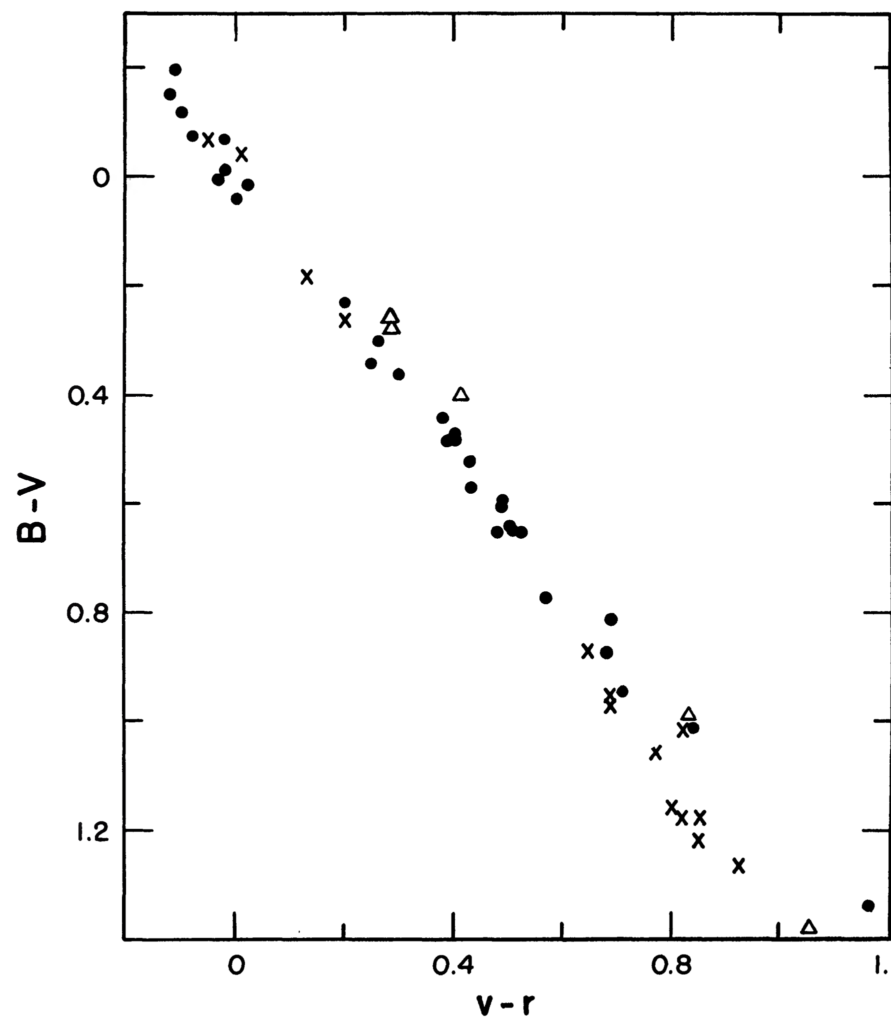

FIG. 3.—Correlation of $(B - V)$ and $(v - r)$ for stars of Tables 1 and 2 with $\delta(U - B) < 0^m.05$. Closed circles are luminosity class IV and V stars, crosses are luminosity class III stars, and triangles are luminosity class I stars.

TABLE 2

FOUR-COLOR DATA FOR SELECTED SUBDWARFS AND OTHER STARS

Name (1)	α 1950 (2)	δ 1950 (3)	$(U-B)_{20}$ (4)	$(B-V)_{20}$ (5)	$(v-r)_{20}$ (6)	n (7)	$\delta(U-B)$ (8)	$(U-B)_c$ (9)	$(B-V)_c$ (10)	$(v-r)_c$ (11)
− 9° 122	$0^h36^m.0$	− 8° 35′	−0.16	0.47	0.44	3	+0.17	0.13	0.60	0.47
+71° 31	0 40 .3	+71 54	−0.19	0.43	0.45	3	+0.19	0.09	0.56	0.47
HD 16031	2 31 .8	−12 36	−0.23	0.44	0.41	3	+0.23	0.14	0.60	0.45
HD 17925	2 50 .1	−12 58	+0.55	0.87	0.68	2	+0.03	(0.67)	(0.91)	0.71
HD 19445	3 05 .5	+26 09	−0.24	0.47	0.45	2	+0.25	0.19	0.65	0.50
HD 22879	3 37 .8	−03 22	−0.10	0.56	0.47	1	+0.19	0.26	0.70	0.52
HD 151877	16 46 .8	+37 06	+0.44	0.83	0.66	1	+0.06	(0.65)	(0.90)	0.71
HD 152792	16 52 .0	+42 55	+0.07	0.64	0.53	1	+0.11	0.30	0.73	0.57
HD 157089	17 18 .6	+01 29	+0.10	0.59	0.49	1	+0.02	0.14	0.61	0.49
+18° 3407	17 33 .1	+18 55	+0.48	0.81	0.69	1	−0.03	(0.38)	(0.77)	0.67
+ 2° 3375	17 37 .3	+ 2 26	−0.26	0.48	0.47	1	+0.28	0.23	0.68	0.54
HD 160693	17 37 .9	+37 13	+0.03	0.61	0.52	1	+0.12	0.26	0.70	0.55
− 9° 4604	17 45 .1	− 9 35	−0.04	0.68	0.63	1	+0.27	(0.65)	(0.90)	0.78
+20° 3603	17 52 .8	+20 17	−0.22	0.43	0.40	1	+0.22	0.11	0.58	0.43
HD 163810*	17 55 .9	−13 05	−0.29*	0.62	0.53	1	+0.45*	....	....	....
HD 175305	18 48 .5	+74 40	+0.14	0.77	0.64	3	+0.23	(0.78)	(0.97)	0.79
− 4° 4617	18 51 .9	− 4 40	−0.07	0.59	0.52	1	+0.19	0.31	0.74	0.58
−15° 5243	19 05 .1	−15 19	−0.05	0.60	0.48	1	+0.18	0.32	0.74	0.54
+26° 3578	19 30 .4	+26 15	−0.21	0.40	0.41	3	+0.22	0.06	0.53	0.42
HD 187923	19 49 .7	+11 30	+0.15	0.65	0.52	2	+0.04	0.23	0.68	0.53
+10° 4091	19 52 .8	+10 36	−0.13	0.60	0.53	2	+0.26	0.44	0.81	0.64
HD 193664	20 17 .0	+66 42	+0.06	0.60	0.49	2	+0.07	0.19	0.65	0.50
+ 5° 4481	20 17 .9	+ 5 53	−0.02	0.62	0.53	3	+0.18	0.38	0.77	0.60
AC 25° 67928	20 22 .6	+24 54	−0.19	0.49	0.50	2	+0.21	0.19	0.65	0.55
HD 195636	20 30 .1	− 9 32	−0.03	0.59	0.57	2	+0.15	0.26	0.70	0.61
HD 203454	21 19 .1	+40 08	−0.03	0.52	0.46	1	+0.08	0.12	0.59	0.47
+17° 4708	22 09 .1	+17 51	−0.20	0.45	0.47	1	+0.20	0.14	0.60	0.50
G 18-39	22 16 .1	+ 8 11	−0.17	0.47	0.51	1	+0.18	0.14	0.61	0.54
− 0° 4470	23 07 .0	+00 28	−0.01	0.73	0.61	3	+0.31	....	....	....
+38° 4955	23 11 .3	+39 09	−0.18	0.69	0.64	3	+0.42	....	....	....
HD 219617	23 14 .5	−14 06	−0.18	0.47	0.43	3	+0.19	0.15	0.61	0.46
+59° 2723	23 24 .2	+60 20	−0.38	0.31	0.42	2	+0.44	....	....	....

*U−B probably wrong. Roman (1955) gives U−B = −0.06, B−V = 0.62.

where η is the integrated blocking coefficient taken over all wavelengths (see WBSB eq. [6]). The change in r due to the removal of all Fraunhofer lines from a star, considering only the back-warming term, is given by

$$\Delta r = 2.5 \log \frac{\int_0^\infty S(\lambda) F_1(\lambda) d\lambda}{\int_0^\infty S(\lambda) F_2(\lambda) d\lambda}, \tag{4}$$

where $F_1(\lambda)$ and $F_2(\lambda)$ are the emergent continuum fluxes from model atmospheres at effective temperatures T_1 and T_2 and $S(\lambda)$ is the spectral response of the system.

Table 3 shows Δr for the eight calibrating stars calculated from equation (4) with F_1 and F_2 given by the black-body distribution. Numerical calculations using the de Jager and Neven (1957) model atmospheres at T_1 and T_2 show that the black-body function is a

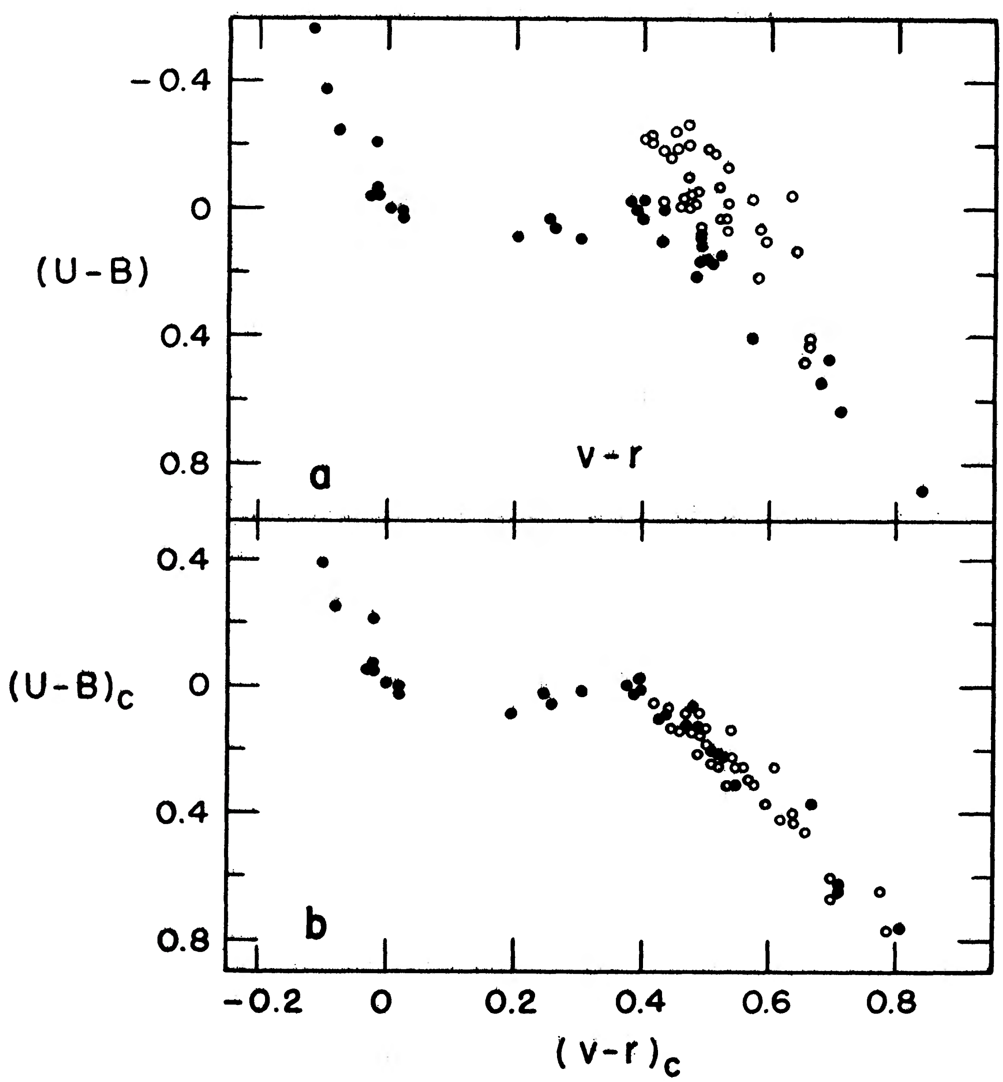

FIG. 4.—*a:* The $(U - B)$, $(v - r)$ two-color diagram for all stars of luminosity classes IV, V, and the subdwarfs in Tables 1 and 2. Closed circles are stars with $\delta < 0^m\!.05$. Open circles are stars with $\delta \geq 0^m\!.05$. *b:* Same as *a*, but with differential blanketing vectors $\Delta(B - V)$ and $\Delta(v - r)$ applied to each star, as discussed in the text.

TABLE 3

DATA FOR STARS USED TO CALIBRATE $\Delta(v-r)$

Star (1)	T_1 °k (2)	T_2 °k (3)	ΔV* (4)	Δr* (5)	$\Delta(v-r)$* (6)	$\Delta(B-V)$* (7)	$\frac{\Delta(v-r)}{\Delta(B-V)}$ (8)	$(B-V)_H$ (9)	$\frac{\Delta r}{\Delta(B-V)}$ (10)
σ Boo†	6800	6700	+0.07	+0.054	+0.016	−0.07	−0.229	0.420	−0.771
π^3 Ori	6750	6650	+0.05	+0.055	−0.005	−0.12	+0.042	0.465	−0.458
110 Her	6550	6400	+0.09	+0.087	+0.003	−0.13	−0.023	0.465	−0.669
ξ Peg†	6421	6270	+0.045	+0.091	−0.046	−0.065	+0.708	0.545	−1.40
50 And	6321	6150	+0.066	+0.107	−0.041	−0.113	+0.363	0.550	−0.947
β Com	6100	5950	+0.06	+0.100	−0.040	−0.16	+0.250	0.60	−0.625
Sun (Melbourne)	6201	6000	+0.09	+0.131	−0.041	−0.17	+0.241	0.645	−0.771
Sun (WBSB)	6201	6000	+0.099	+0.131	−0.032	−0.157	+0.204	0.645	−0.834
51 Peg	5800	5600	+0.08	+0.148	−0.068	−0.20	+0.340	0.70	−0.740
HD 19445	....	....	....	....	....	....	+0.234	0.61	−0.866

*The sign of the tabulated magnitude or color differences refers to the effect on the measured colors of a strong-line star as lines are removed. Positive signs mean that the magnitudes get fainter or that the colors get redder.

†ξ Peg discarded in the least squares fit. σ Boo given half weight.

good approximation for the present problem. The ΔV values of Table 3 are taken directly from Table 3*A* of WBSB, and these values, combined with Δr, give the $\Delta(v - r)$ value of column 6 in Table 3, which is the correction to $v - r$ if all the lines are removed from the stars in question. The $\Delta(v - r)$ values are considerably smaller than $\Delta(B - V)$ given in column 7 (and taken from Table 3*A* of WBSB), but they are not negligible. Column 8 gives $\Delta(v - r)/\Delta(B - V)$, which is a function of the $B - V$ color, hereafter called "$(B - V)_H$," which the stars would have if they had Hyades-like metal abundance.

Figure 6 shows the correlation of $\Delta(v - r)/\Delta(B - V)$ with $(B - V)_H$ obtained from these data. The closed circles are the calibrating stars already discussed, while the triangle is the well-known subdwarf HD 19445. The lines are so weak for this star that $T_1 \simeq T_2$, and the change in the colors is vanishing small when the remaining lines are completely removed. Hence a new procedure was used to obtain $\Delta(v - r)/\Delta(B - V)$. The observed $B - V$ color of HD 19445 is $B - V = 0.46$, which, when corrected by $\Delta(B - V) = 0^m.15$ to bring this star to the Hyades two-color diagram, gives $(B - V)_H = 0.61$ (see WBSB, Table 3*B*). Figure 3 shows that Hyades-like stars (*the closed circles*) have $v - r = +0.485$ at $(B - V)_H = +0.61$, but, since the observed $v - r$ for HD 19445 is $+0.45$, it is apparent that $\Delta(v - r) = 0.035$. Consequently, $\Delta(v - r)/\Delta(B - V) = 0.035/0.15 = 0.234$. But it must be emphasized that this value is not determined in a fundamental manner because it assumes that the subdwarfs will no longer be segregated from Hyades-like stars when the proper blanketing corrections are applied, and this is the point we wish to prove. But the remarkable agreement of the triangle with the closed circles in Figure 6 shows that $\Delta(v - r)/\Delta(B - V)$ determined in this way is correct—which anticipates the result, now to be shown, that the subdwarf points mingle with the Hyades-like stars in the color-color diagrams of Figures 4 and 5 when these theoretical blanketing corrections are applied.

A least-squares fit to the points of Figure 6, with ξ Peg discarded and σ Boo given half-weight, is

$$\frac{\Delta(v - r)}{\Delta(B - V)} = \underset{\pm 0.190}{1.469}(B - V)_H - \underset{\pm 0.110}{0.664} \qquad \text{for } 0.4 < (B - V)_H < 0.7\,. \tag{5}$$

In a similar fashion, the correction to the r magnitude can be found by using the data of columns 9 and 10 of Table 3, with the result

$$\frac{\Delta r}{\Delta(B - V)} = -\underset{\pm 0.257}{0.647}(B - V)_H - \underset{\pm 0.149}{0.368}\,. \tag{6}$$

Equations (5) and (6) complete the formalism needed to correct for blanketing in r and in $v - r$. The practical steps are as follows: (1) Determine $\delta(U - B)$ relative to the Hyades $U - B$, $B - V$ diagram [see Fig. 5 of WBSB for the definition of $\delta(U - B)$]. (2) Enter Table 4 of WBSB to find ΔV, $\Delta(U - B)$, and $\Delta(B - V)$. (3) Add $\Delta(B - V)$ to the observed $B - V$ to obtain $(B - V)_H$ [note that $(B - V)_H$ is sometimes called $(B - V)_c$, which denotes "corrected value"]. (4) Use equations (5) and (6) to compute $\Delta(v - r)$ and Δr and apply these corrections to the observed values to reduce them to Hyades-like stars.

An example will illustrate the procedure. Consider BD$-9°122$ of Table 2, which has an ultraviolet excess of $\delta(U - B) = 0^m.17$ and observed colors of $U - B = -0.16$, $B - V = 0.47$, $v - r = 0.44$. Table 4 of WBSB gives $\Delta(U - B) = 0.29$, and $\Delta(B - V) = 0.13$; hence $(U - B)_c = 0.13$, and $(B - V)_c = 0.60$. Equation (5) then gives $\Delta(v - r)/\Delta(B - V) = 0.22$, or $\Delta(v - r) = 0.03$, which finally gives $(v - r)_c = 0.47$.

At this point it is well to emphasize that the foregoing procedure is based on the previous measurement (WBSB, Table 1) of the $\epsilon(\lambda)$ blocking coefficients of the calibrating

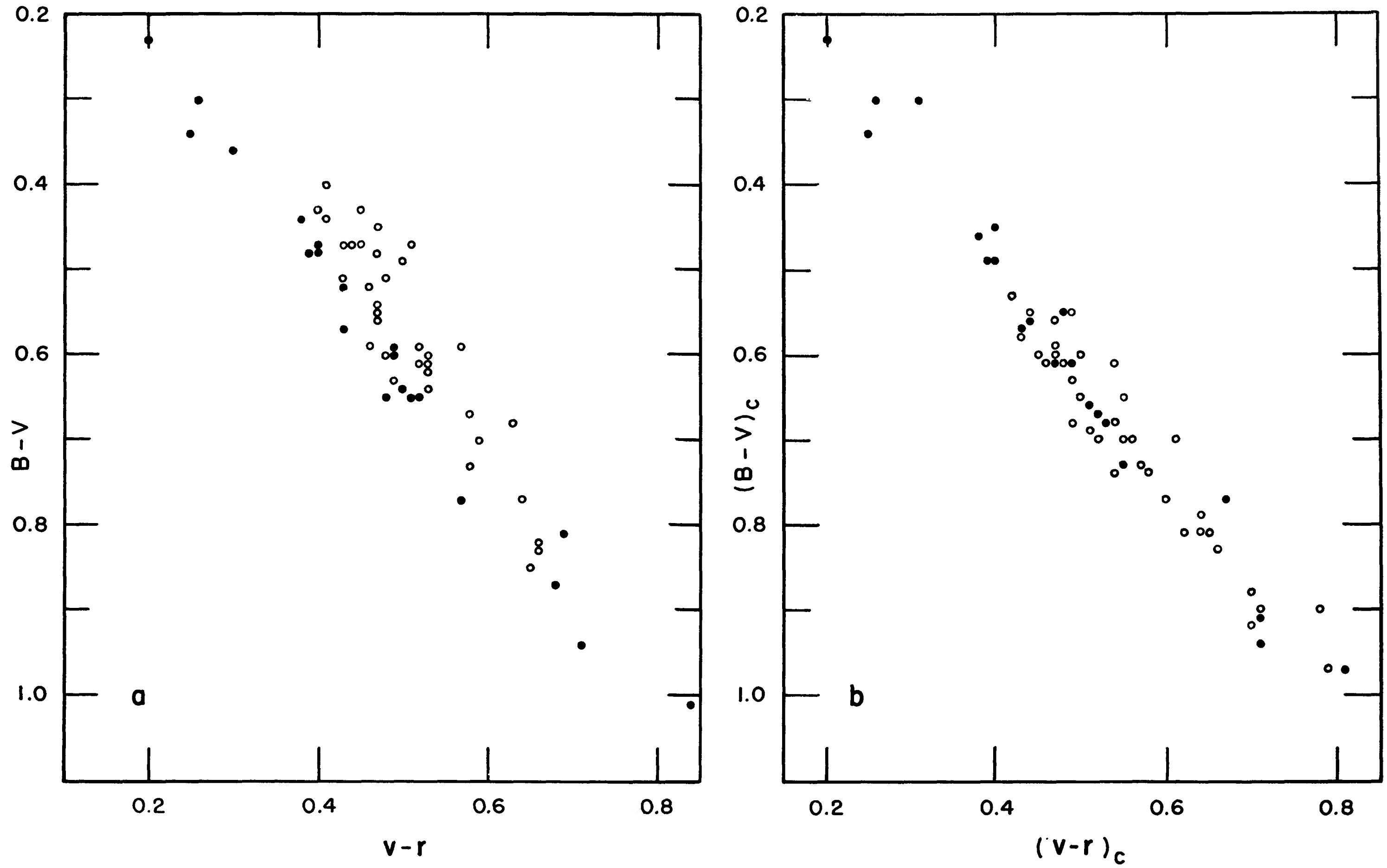

FIG. 5.—*a:* The $(B - V)$, $(v - r)$ two-color diagram for the same stars with the same symbols as in Fig. 4. *b:* Same as *a* but with differential blanketing vectors $\Delta(B - V)$ and $\Delta(v - r)$ applied to each star.

stars, together with the condition that the stars correct to the Hyades $U - B$, $B - V$ diagram. It is not based on the premise that stars with large $\delta(U - B)$ values should define the same $B - V$, $v - r$ two-color relation as Hyades-like stars.

The results of applying the blanketing corrections to all stars of Tables 1 and 2 of luminosity class IV and V and the subdwarfs are shown in Figures 4, *b*, and 5, *b*. Several of the standards of Table 1 have appreciable $\delta(U - B)$ values, and the corrections have also been applied to them. The remarkable fact emerges that the line-blanketing corrections appear to eliminate the segregation of strong- and weak-lined stars in the two-color diagrams. We have taken this to mean that the well-known anomalous energy distribution of subdwarfs can now be explained over the range of λ 3600 A to λ 6700 A as due principally to the effects of the weak Fraunhofer lines.

V. THE BLANKETING EFFECT IN THE STEBBINS-WHITFORD $G - I$ INDEX

Equation (5) and Figure 6 show that, although $\Delta(v - r)$ is much smaller than $\Delta(B - V)$, it is not zero. Therefore, observation of stars in the halo globular clusters, which are known to have weak lines and $\delta(U - B)$ values of about $0^{m}_{.}20$, will still require corrections of $\Delta(v - r) \simeq 0^{m}_{.}03$ to $\Delta(v - r) \simeq 0^{m}_{.}04$ for differential line blanketing relative to the Hyades. This correction is, of course, much smaller than $\Delta(B - V) \simeq 0^{m}_{.}18$ required in the conventional V, $B - V$ color-magnitude diagrams, but it is not zero.

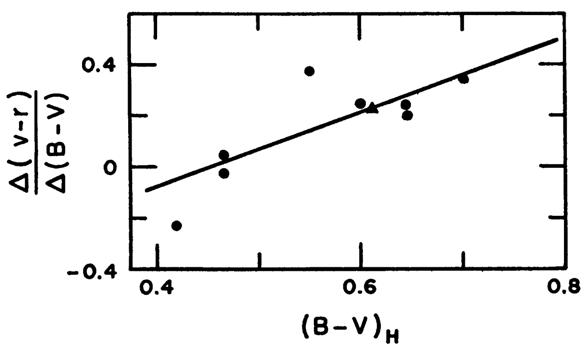

FIG. 6.—The correlation of $\Delta(v - r)/\Delta(B - V)$ with $(B - V)_H$ defined in the text The triangle represents the extreme subdwarf HD 19445. The closed circles are stars from Table 3

It is therefore of interest to compute the blanketing correction in the Stebbins-Whitford $G - I$ system, where the effective wavelengths of the band passes are approximately $\bar{\lambda}_G \simeq 5700$ A, $\bar{\lambda}_I \simeq 10300$ A. Again we have assumed that the blocking effect of the lines in I is negligible because of the very few Fraunhofer lines in this spectral region and therefore that ΔI arises solely from the back-warming term. Table 4 gives $\Delta(G - I)$ for the eight calibrating stars previously discussed. The back-warming term in both ΔG and ΔI was computed by equation (4), using the sensitivity function of the G and I bands tabulated by Stebbins and Whitford (1943) and again using black-body functions for F_1 and F_2. Columns 4 and 7 give the back-warming results, where, as usual, as lines are removed from a star, the continuum level drops and both G and I become fainter.

The G filter band is very close to the conventional visual magnitude V and is affected by blocking in addition to back-warming. The blocking in G is listed in column 5 of Table 4 and is taken directly from Table 2 of WBSB or from Melbourne's data (1960), but with $0^{m}_{.}01$ subtracted because G is slightly further to the red than V. The only exceptions are σ Boo, π^3 Ori, and 110 Her, where ΔV (blocking) is very small and it was assumed that ΔG (blocking) $= \Delta V$ (blocking). The total ΔG (blocking plus back-warming) is given in column 6. The resulting effect on the $G - I$ colors caused by the removal of all the lines is given in column 8, where it is seen that $\Delta(G - I)$ is nearly zero. Finally, col-

110 Her	6550	6400	+0.102	−0.03	+0.072	+0.063	+0.009	−0.13	−0.069	0.465
ξ Peg	6421	6270	+0.107	−0.054	+0.053	+0.065	−0.012	−0.065	+0.185	0.545
50 And	6321	6150	+0.125	−0.057	+0.068	+0.076	−0.008	−0.113	+0.071	0.550
β Com	6100	5950	+0.117	−0.05	+0.067	+0.071	−0.004	−0.16	+0.025	0.60
Sun (Melbourne)	6201	6000	+0.153	−0.06	+0.093	+0.093	−0.000	−0.17	0.000	0.645
Sun (WBSB)	6201	6000	+0.153	−0.064	+0.089	+0.093	−0.004	−0.157	+0.025	0.645
51 Peg	5800	5600	+0.173	−0.07	+0.103	+0.104	−0.001	−0.20	+0.005	0.70

*The sign of the tabulated magnitude or color difference refers to the effect on the measured colors of a strong-line star as lines are removed. Positive signs mean that the magnitudes get fainter or that the colors get redder.

TABLE 4

DATA FOR STARS USED TO CALIBRATE $\Delta(G-I)$

Star	T_1 °k	T_2 °k	ΔG^* Bckwm.	ΔG^* Blocking	ΔG^* Total	ΔI^* Bckwm.	$\Delta(G-I)^*$	$\Delta(B-V)^*$	$\frac{\Delta(G-I)}{\Delta(B-V)}$	$(B-V)_H$
(1)	(2)	(3)	(4)	(5)	(6)	(7)	(8)	(9)	(10)	(11)
σ Boo	6800	6700	+0.063	−0.01	+0.053	+0.039	+0.014	−0.07	−0.200	0.420
π^3 Ori	6750	6650	+0.064	−0.03	+0.034	+0.039	−0.005	−0.12	+0.042	0.465

umn 10 gives $\Delta(G-I)/\Delta(B-V)$, which is plotted in Figure 7 against the $(B-V)_H$ of column 11. This diagram clearly shows that $\Delta(G-I)$ is negligible for $0.4 < (B-V)_H < 0.7$. The least-squares line passing through the points of Figure 7 is

$$\frac{\Delta(G-I)}{\Delta(B-V)} = \underset{\pm 0.150}{0.284}(B-V)_H - \underset{\pm 0.087}{0.151}\,. \qquad (7)$$

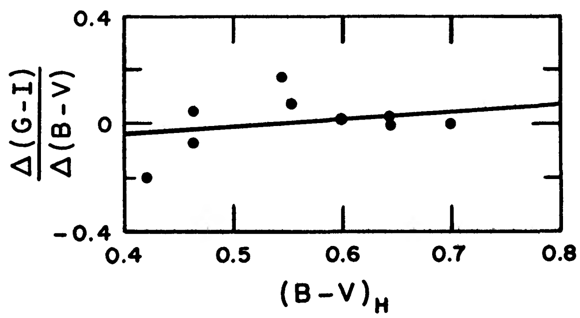

FIG 7—The correlation of $\Delta(G-I)/\Delta(B-V)$ with $(B-V)_H$

VI. CONCLUSION

The results of the original discussion of Sandage and Eggen (1959), of WBSB, and, finally, of the present study show that line-blanketing effects are strongest for the shortest wavelengths and decrease markedly toward the red. The principal result can be summarized by tabulating the corrections $\Delta(U-B)$, $\Delta(B-V)$, $\Delta(v-r)$, and $\Delta(G-I)$ which must be applied to observed $U-B$, $B-V$, $v-r$, and $G-I$ colors of a typical extreme subdwarf, such as is encountered near the main-sequence termination point of a halo globular cluster, to reduce the colors to Hyades-like stars. These stars have observed colors of $B-V = 0.45$ and $U-B = -0.24$, which gives $\delta(U-B) = 0^{m}.24$, which, when fed through the correction procedure, yields $\Delta(U-B) = 0.40$, $\Delta(B-V) = 0.18$, $\Delta(v-r) = 0.04$, and $\Delta(G-I) = 0.00$. These numbers clearly show the desirability of observing weak-lined stars in the red spectral regions so as to minimize the blanketing corrections.

REFERENCES

Code, A D. 1959, *Ap J.*, **130**, 473.
Gehrels, T , and Teska, T. M 1960, *Pub. A S.P.*, **72**, 115
Jager, C de, and Neven, L. 1957, *Ann Obs R. Belge* , Vol **8**.
Johnson, H L , and Harris, D. L 1954, *Ap J* , **120**, 196
Johnson, H L , and Morgan, W. W. 1953, *Ap J* , **117**, 313.
Kasha, M 1948, *J Opt Soc America*, **38**, 929.
Matthews, T. A., and Sandage, A 1963, *Ap. J* , in press
Melbourne, W. G. 1960, *Ap J* , **132**, 101.
Roman, N G. 1955, *Ap J. Suppl.*, **2**, 195.
Sandage, A. R. 1963, *Ap J* , in press.
Sandage, A. R., and Eggen, O. J. 1959, *M N* , **119**, 278.
Smak, J. 1960, *Acta Astr* , **10**, 167
Stebbins, J., and Whitford, A. E 1943, *Ap. J* , **98**, 20.
Wildey, R. L , Burbidge, E. M , Sandage, A. R , and Burbidge, G. R 1962, *Ap J* , **135**, 94.